Optimum Finite-Length Equalization for Multicarrier Transceivers

Naofal Al-Dhahir, *Member, IEEE,* and John M. Cioffi, *Senior Member, IEEE*

***Abstract*— A *new* criterion for partially-equalizing severe-ISI channels to reduce the cyclic prefix overhead of the discrete multitone (DMT) transceiver, assuming a fixed transmission bandwidth, is introduced. The equalized DMT is shown to recover a significant portion of the performance loss incurred because of the use of a moderate-size FFT in the DMT to reduce latency and implementation cost. In particular, equalizers designed using our new criterion result in a higher DMT performance margin than traditional mean-square-error DMT equalizers. Finally, additional promising methods that further enhance the performance of the equalized DMT are investigated.**

I. Introduction

MULTICARRIER modulation (MCM) has been recently demonstrated to be a viable technology for high-speed data transmission over spectrally shaped noisy channels. Modems designed using the MCM principle parse, using an orthogonal transformation, the channel spectrum (which could exhibit wide variations over the transmission bandwidth) into a large number of parallel, independent, and flat subchannels. The optimum orthogonal transformation is based on the eigendecomposition of a channel-and-noise-dependent matrix [13], which under the assumption of a large number of subchannels causes the MCM transceiver to achieve close-to-optimum performance levels.

To avoid the formidable costs associated with the eigendecomposition of a large matrix, another form of MCM, called the discrete multitone (DMT), that uses the computationally-efficient fast Fourier transform (FFT) to create the independent subchannels was proposed in [8]. When combined with bandwidth optimization and optimization of the bit distribution across the usable subchannels, the performance of the FFT-based MCM transceiver becomes very close to that of the optimum eigendecomposition-based MCM transceiver.

To ensure independence of the subchannels for a finite N-point FFT, every input block of size N is prefixed with a sequence of symbols whose length is equal to the channel memory such that the input sequence looks periodic to the channel. The periodicity of the input renders the channel-description matrix *circulant*, making the FFT basis vectors identical to the channel eigenvectors (assuming white noise).

For highly dispersive channels, the length of the cyclic prefix is large resulting in an appreciable bit rate loss, especially for a moderate FFT size. In this paper, we investigate the use of equalization to reduce the cyclic prefix overhead by optimally shortening the channel impulse response duration. In particular, *we derive the optimum equalization criterion in conjunction with the DMT.* We demonstrate that our proposed equalized-DMT system is a valuable solution to the problem of approaching theoretical performance levels under practical complexity constraints.

The rest of this paper is organized as follows. In Section II, after a brief overview of the DMT transceiver, we derive the optimum equalization criterion for the DMT and show how to compute the equalizer settings under this criterion. Simulation results that compare the performance of the equalized DMT, under our new criterion and a previously-used criterion, with a theoretical performance upperbound and the case of no equalization are presented in Section III. Finally, in Section IV, we describe several measures that could result in an additional performance improvement for the equalized-DMT system.

II. A New Equalization Criterion for the DMT

A. System Model

A block diagram of the basic DMT transceiver is depicted in Fig. 1. An input bit stream of rate R_{DMT} (b/s) is buffered into blocks of $b_{DMT} = R_{DMT}T$ bits, where T is the multicarrier symbol period. These b_{DMT} bits are distributed optimally across $\bar{N} \leq \frac{N}{2}$ subchannels. The bits assigned to the ith subchannel, b_i, are mapped by the DMT encoder to the ith complex subsymbol of the kth transmitted symbol, which is denoted by $X_{i,k}$. These $\bar{N}$ complex subsymbols are then transformed by an N-point IFFT into N *real* samples by imposing the Hermitian symmetry condition $X_{i,k} = X^*_{N-i,k}$ $(1 \leq i \leq N)$. The N samples are then converted from parallel to serial format and applied, after adding a cyclic prefix and passing them through a digital-to-analog converter (DAC) and a low-pass filter, to the channel $h(t)$. In this paper, we shall exclusively deal with the equivalent discrete-time representation of the channel, which will be assumed an FIR filter with $(\nu+1)$ taps, i.e., $h(D) = h_0 + h_1 D + \cdots + h_\nu D^\nu$. At the receiver, the output signal is first low-pass filtered and sampled, then the cyclic prefix is removed. The resultant N real output samples are converted to parallel format and

Paper approved by J. H. Winters, the Editor for Equalization of the IEEE Communications Society. Manuscript received February 8, 1994; revised January 24, 1995. This work was supported by NSF under Contract NCR-9203131, JSEP under Contract DAAL 03-91-C-0010, and NASA under Contract NAG2-842. This paper was presented in part at Globecom'94 in San Francisco, November 1994.

N. Al-Dhahir was with the Information Systems Laboratory, Stanford University, Stanford, CA 94305-4055 USA. He is now with the GE Corporate R&D Center, Schenectady, NY 12301 USA.

J. M. Cioffi is with the Information Systems Laboratory, Department of Electrical Engineering, Stanford University, Stanford, CA 94305-4055 USA.

Publisher Item Identifier S 0090-6778(96)00810-0.

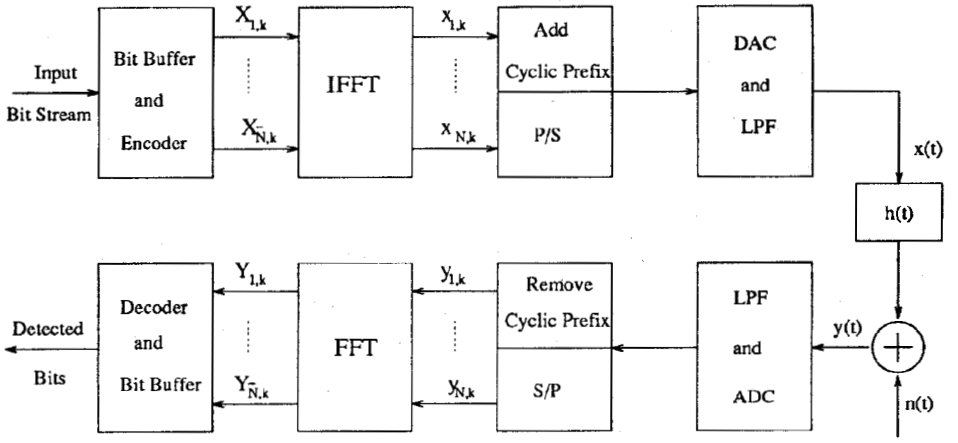

Fig. 1. Block diagram of the DMT transceiver (P/S and S/P mean parallel-to-serial and serial-to-parallel converters, respectively).

then transformed, through an N-point FFT, to $\bar{N}$ complex subsymbols that are individually decoded.

B. Equalization for the DMT

In the DMT, an N-point FFT is used to divide the channel spectrum into $\bar{N}$ subchannels. Strictly speaking, N has to be infinite for the subchannels to be independent and memoryless. On the other hand, to reduce the implementation cost, N has to be finite (preferably a power of 2 and not larger than 512). The use of a finite input blocklength on ISI channels results in interblock interference (IBI) which degrades performance significantly. To eliminate IBI in the DMT, the ν last input samples in each input block of length N are repeated at the beginning of the block. This makes the input sequence look periodic and clears the channel memory at the end of each input block making successive block transmissions independent.

However, on severe-ISI channels (i.e., channels with large ν), adding the cyclic prefix results in a bit rate reduction by a factor of $\frac{\nu}{N+\nu}$, which could be quite significant, even for a moderate FFT size.

An elegant solution to this problem was suggested in [6] and [7] where the authors proposed to linearly equalize the channel impulse response (CIR), denoted by the vector $\mathbf{h} \stackrel{\text{def}}{=} [h_0 \quad \cdots \quad h_\nu]$ which is of length $(\nu+1)$, to a much shorter target impulse response (TIR) of length (N_b+1), thus improving the bit rate by a factor of $(1+\frac{(\nu-N_b)}{N+N_b})$. In [6] and [7], the TIR was not a fixed partial response (as it is usually assumed for equalized maximum likelihood (ML) detection using the Viterbi algorithm). Instead, it is chosen as the impulse response of length (N_b+1) that is closest, in the mean square sense, to the combined-channel-equalizer impulse response.

More specifically, referring to Fig. 2, the time-domain equalizer (TEQ) and TIR coefficients are chosen to minimize the mean square of the error sequence $e_k \stackrel{\text{def}}{=} z_k - r_k$. Under the assumptions of a length-N_f TEQ denoted by the vector $\mathbf{w} = [w_0 \quad \cdots \quad w_{N_f-1}]^t$ (where $(.)^t$ denotes the transpose), a unit-energy constraint (UEC) on the TIR $\mathbf{b} \stackrel{\text{def}}{=} [b_0 \quad \cdots \quad b_{N_b}]$,

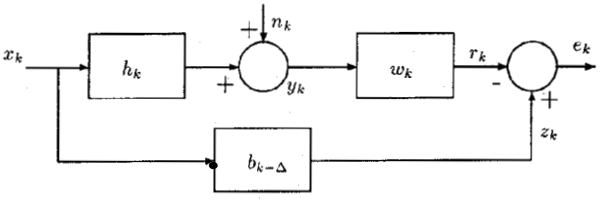

Fig. 2. Block diagram of the TEQ.

and uncorrelated input symbols, it was shown in [11] and [4] that the optimum TIR, $\mathbf{b}_{opt.}$, is equal to the unit-norm eigenvector that corresponds to the minimum eigenvalue of the channel-and-noise-dependent matrix $\mathbf{R}_\Delta$ defined as follows

$$\mathbf{R}_\Delta \stackrel{\text{def}}{=} [\mathbf{0}_{(N_b+1)\times\Delta} \quad \mathbf{I}_{N_b+1} \quad \mathbf{0}_{(N_b+1)\times s}] \left(\frac{1}{S_x}\mathbf{I}_{N_f+\nu} + \mathbf{H}^*\mathbf{R}_{nn}^{-1}\mathbf{H}\right)^{-1} \begin{bmatrix} \mathbf{0}_{\Delta\times(N_b+1)} \\ \mathbf{I}_{N_b+1} \\ \mathbf{0}_{s\times(N_b+1)} \end{bmatrix} \quad (1)$$

where $\mathbf{0}_{m\times n}$ is the $m\times n$ null matrix, $\mathbf{I}_m$ is the identity matrix of size m, $(.)^*$ denotes the complex-conjugate transpose, Δ is the equalizer delay $(0 \le \Delta \le N_f+\nu-N_b-1)$, $s \stackrel{\text{def}}{=} N_f+\nu-\Delta-N_b-1$, S_x is the average energy of the input symbols, $\mathbf{R}_{nn}$ is the N_f-dimensional noise-correlation matrix, and $\mathbf{H}$ is an $N_f \times (N_f+\nu)$ channel matrix given by

$$\mathbf{H} = \begin{bmatrix} h_0 & h_1 & \cdots & h_\nu & 0 & \cdots & 0 \\ 0 & h_0 & h_1 & \cdots & h_\nu & 0 & \cdots \\ \vdots & & \ddots & \ddots & & \ddots & \vdots \\ 0 & \cdots & 0 & h_0 & h_1 & \cdots & h_\nu \end{bmatrix}.$$

Once $\mathbf{b}_{\text{opt.}}$ is determined, the minimum-mean-square-error unit-energy-constrained (MMSE-UEC) TEQ coefficients are calculated from [2]

$$\mathbf{w}^*_{\text{opt.}} = [\mathbf{0}_{1\times\Delta} \quad \mathbf{b}^*_{\text{opt.}} \quad \mathbf{0}_{1\times s}]\mathbf{H}^*\left(\mathbf{H}\mathbf{H}^* + \frac{\mathbf{R}_{nn}}{S_x}\right)^{-1}. \quad (2)$$

By optimizing the TEQ and TIR coefficients, the equalized-DMT transceiver achieves high performance (since it eliminates IBI with a much shorter cyclic prefix overhead) and low

implementation cost (because of the moderate FFT size and equalizer length used). Indeed, as we shall show in Section III, the performance of the equalized-DMT transceiver, when its parameters are chosen properly, can get very close to theoretical performance limits.

C. The Geometric SNR

Although the mean square error (MSE) is the most popular equalization criterion since it is easy to analyze and since it lends itself to a simple adaptive implementation (the performance surface has a unique global optimum), we shall argue next that it is not the optimum equalization criterion in conjunction with the DMT.

Assuming that the subchannels of the DMT are equally spaced (each assumed to be of width $\frac{1}{T}$ Hz), independent, and memoryless, then the total number of bits transmitted in one DMT symbol is given by

$$\begin{aligned} b_{DMT} &= \sum_{i=1}^{\bar{N}} b_i \\ &= \sum_{i=1}^{\bar{N}} \log_2\left(1+\frac{SNR_i}{\Gamma_i}\right). \end{aligned} \tag{3}$$

SNR_i is the signal-to-noise ratio of the ith subchannel and is defined by $SNR_i \stackrel{\text{def}}{=} \frac{S_{x,i}|H_i|^2}{R_{nn,i}}$ where $S_{x,i}$, $R_{nn,i}$, and $|H_i|^2$ are the input energy, noise power spectral density (psd), and channel gain of the ith subchannel. Γ_i is the gap [10] that characterizes the distance (in dB) between SNR_i and the SNR required to achieve capacity, and is a function of the assumed probability of error. We shall assume that all subchannels are required to maintain the same probability of error, which results in $\Gamma_i = \Gamma$ for all subchannels. It was shown in [10] that $\Gamma \approx \frac{\gamma_m}{3\gamma_{\text{eff}}}(Q^{-1}(\frac{P_e}{2}))^2$, where γ_m is the desired system margin, γ_{eff} is the effective coding gain of any applied code, P_e is the assumed constant symbol error rate (for a QAM signal constellation) across the subchannels, and $Q(x) \stackrel{\text{def}}{=} \int_x^\infty e^{-\frac{u^2}{2}}du$. In addition, we shall assume a flat input energy distribution across the subchannels,[1] in which case $SNR_i = \frac{S_x|H_i|^2}{R_{nn,i}}$.

Equation (3) can be expressed as follows

$$b_{DMT} = \bar{N}\log_2\left(1+\frac{SNR_{\text{geom}}}{\Gamma}\right) \tag{4}$$

where the *geometric SNR* is defined by

$$SNR_{\text{geom}} \stackrel{\text{def}}{=} \Gamma\left\{\left[\prod_{i=1}^{\bar{N}}\left(1+\frac{SNR_i}{\Gamma}\right)\right]^{\frac{1}{\bar{N}}} - 1\right\}. \tag{5}$$

For the purposes of this paper, we shall assume that the input power level and the sampling frequency are chosen such that the number of usable subchannels $\bar{N} = \frac{N}{2}$ (i.e., all the available bandwidth is used). Furthermore, the "1+" and "−1" terms can be typically ignored, simplifying (5) to

$$SNR_{\text{geom}} \approx \left[\prod_{i=1}^{\bar{N}}(SNR_i)\right]^{\frac{1}{\bar{N}}}. \tag{6}$$

This expression makes the name "geometric SNR" obvious.

Using (4), we can compute the achievable bit rate of the DMT as follows

$$\begin{aligned} R_{DMT} &\stackrel{\text{def}}{=} \frac{b_{DMT}}{T}\frac{N}{(N+N_b)} \\ &= \frac{b_{DMT}f_s}{N}\frac{N}{(N+N_b)} \\ &= \frac{f_s}{(N+N_b)}\bar{N}\log_2\left(1+\frac{SNR_{\text{geom}}}{\Gamma}\right) \end{aligned} \tag{7}$$

where f_s is the sampling frequency.

Therefore, assuming a fixed transmission bandwidth, maximizing the achievable bit rate of the DMT is equivalent to maximizing its geometric SNR.

For the equalized DMT, the geometric SNR is approximately given by

$$SNR_{\text{geom}} \approx S_x\left[\prod_{i=1}^{\bar{N}}\left(\frac{|B_i|^2}{R_{nn,i}|W_i|^2}\right)\right]^{\frac{1}{\bar{N}}} \tag{8}$$

where B_i and W_i are the ith FFT coefficients of the TIR and the TEQ, respectively.

Choosing $\mathbf{w}$ and $\mathbf{b}$ to minimize the mean square of the equalizer error sequence does not necessarily maximize (8). Instead, we propose to use the $(\mathbf{b},\mathbf{w})$ combination that maximizes SNR_{geom} to optimize the performance of the equalized DMT. In the sequel, we shall refer to this equalizer by the name geometric TEQ.

D. Computing the Optimum Geometric TEQ Settings

Computing the optimum settings of the geometric TEQ is a two-step procedure. First, we need to compute the coefficients of the optimum TIR of a given length (N_b+1) that maximizes SNR_{geom}. Second, we use (2) to compute the coefficients of the length$-N_f$ TEQ that results in the minimum mean square error when equalizing the original CIR to $\mathbf{b}_{\text{opt}}$.

To simplify the optimization procedure, we shall assume that the input SNR is high enough so that we can ignore the dependence of SNR_{geom} on Γ and use the entire available bandwidth, i.e., $\bar{N} = \frac{N}{2}$. In this case, maximizing SNR_{geom} as given by (8) is equivalent to maximizing the cost function $L(\mathbf{b})$ defined as follows[2]

$$L(\mathbf{b}) \stackrel{\text{def}}{=} \frac{1}{\bar{N}}\sum_{i=1}^{\bar{N}}\ln|B_i|^2. \tag{9}$$

[1] This assumption has been shown to result in a negligible performance loss from the case where the shape of the input psd is optimized [3], [9].

[2] This cost function also assumes that the noise at the output of the equalizer is independent of $\mathbf{b}$, which is not exactly accurate [because of the interdependence between $\mathbf{w}$ and $\mathbf{b}$ through (2)], nevertheless, it simplifies the analysis considerably.

Now

$$B_i \stackrel{\text{def}}{=} \sum_{k=0}^{N_b} b_k^* e^{-j\frac{2\pi}{N}ik} \stackrel{\text{def}}{=} \mathbf{b}^* \mathbf{g}_i^{(N_b+1)}$$

where $\mathbf{g}_i^{(N_b+1)} \stackrel{\text{def}}{=} [1 \quad e^{-j\frac{2\pi}{N}i} \quad \cdots \quad e^{-j\frac{2\pi}{N}iN_b}]^t$.

Therefore, (9) becomes

$$L(\mathbf{b}) \stackrel{\text{def}}{=} \frac{1}{\bar{N}} \sum_{i=1}^{\bar{N}} \ln\left(\mathbf{b}^* \mathbf{G}_i^{(N_b+1)} \mathbf{b}\right) \tag{10}$$

where

$$\mathbf{G}_i^{(N_b+1)} \stackrel{\text{def}}{=} \mathbf{g}_i^{(N_b+1)} \mathbf{g}_i^{*(N_b+1)} = \begin{bmatrix} 1 & e^{j\frac{2\pi}{N}i} & \cdots & e^{j\frac{2\pi}{N}iN_b} \\ e^{-j\frac{2\pi}{N}i} & 1 & e^{j\frac{2\pi}{N}i} & \vdots \\ \vdots & \ddots & \ddots & \ddots \\ e^{-j\frac{2\pi}{N}iN_b} & \cdots & e^{-j\frac{2\pi}{N}i} & 1 \end{bmatrix}.$$

To maximize $L(\mathbf{b})$ as determined by (10) while avoiding the impractical solution of an infinite-gain TIR, we need to impose additional constraints on $\mathbf{b}$. One such constraint is the unit-energy constraint $\mathbf{b}^*\mathbf{b} = 1$. However, with this constraint alone, it can be readily checked that the optimum TIR is the memoryless channel, i.e., $|B_i|^2 = 1 \ \forall i$. This requires "full" equalization of the CIR which could result in a large equalization MSE (especially for short TEQ lengths) and is not needed since we are using the DMT to combat ISI!

Therefore, we shall constrain the MSE of the TEQ to remain below a maximum tolerable value, call it $MSE_{\max}$. Using the results of [4], this latter MSE condition is equivalent to

$$\mathbf{b}^* \mathbf{R}_\Delta \mathbf{b} \leq MSE_{\max} \tag{11}$$

where $\mathbf{R}_\Delta$ was defined in (1).

In summary, we want to maximize the Lagrangian

$$L(\mathbf{b}) = \frac{1}{\bar{N}} \sum_{i=1}^{\bar{N}} \ln\left(\mathbf{b}^* \mathbf{G}_i^{(N_b+1)} \mathbf{b}\right) + \lambda(\mathbf{b}^*\mathbf{b} - 1) \tag{12}$$

subject to the constraint $\mathbf{b}^*\mathbf{R}_\Delta\mathbf{b} \leq MSE_{\max}$.

This is a *nonlinear constrained* optimization problem which does not have an analytical closed-form solution for $\mathbf{b}$. However, starting with a certain initial condition for $\mathbf{b}$, we can arrive at a locally-optimum solution using iterative numerical techniques. In this paper, we shall use the *MATLAB optimization toolbox*, which implements sequential quadratic programming (SQP) methods to perform the optimization [1].

Basically, at each iteration of the SQP algorithm, the Hessian of the Lagrangian cost function in (12) is approximated using a quasi-Newton updating procedure. Then, this is used to formulate a quadratic programming subproblem whose solution establishes a search direction for a line search procedure [12].

E. An Upperbound on Performance

An upperbound on SNR_{geom} can be obtained by letting the DMT blocklength and the number of equalizer taps become infinite.[3] This upperbound can be derived as follows

$$\begin{aligned} SNR_{\text{geom}} &\approx \left[\prod_{i=1}^{\bar{N}} \left(\frac{S_x|B_{\text{opt},i}|^2}{R_{nn,i}|W_{\text{opt},i}|^2}\right)\right]^{\frac{1}{\bar{N}}} \\ &\leq e^{\left(\frac{1}{\Omega_{\text{opt}}}\int_0^{\Omega_{\text{opt}}} \ln\left(\frac{S_x|B_{\text{opt}}(f)|^2}{R_{nn}(f)|W_{\text{opt}}(f)|^2}\right)df\right)} \\ &\leq \frac{1}{\Omega_{\text{opt}}}\int_0^{\Omega_{\text{opt}}} \left(\frac{S_x|B_{\text{opt}}(f)|^2}{R_{nn}(f)|W_{\text{opt}}(f)|^2}\right)df \\ &= \frac{1}{\Omega_{\text{opt}}}\int_0^{\Omega_{\text{opt}}} \left(\frac{S_x|H(f)|^2}{R_{nn}(f)}\left(1+\frac{R_{nn}(f)}{S_x|H(f)|^2}\right)^2\right)df \\ &\approx \frac{1}{\Omega_{\text{opt}}}\int_0^{\Omega_{\text{opt}}} \left(\frac{S_x|H(f)|^2}{R_{nn}(f)}\right)df \ : \end{aligned}$$

for high input SNR

where Ω_{opt} is the optimum transmission bandwidth and is equal to $\lim_{N\to\infty} \frac{\bar{N}}{N} f_s$ (which is equal to $\frac{f_s}{2}$ only for high input SNR). Note that the second inequality follows from the definition of the "geometric average" as the blocklength becomes infinite [14], while the third inequality is a well-known relationship between the "geometric average" and the "arithmetic average" of a function [14]. Finally, the fourth line above follows from the relationship between $W_{\text{opt}}(f)$ and $B_{\text{opt}}(f)$ for infinite-length filters, namely that [14], [10]

$$|B_{\text{opt}}(f)|^2 = |W_{\text{opt}}(f)|^2|H(f)|^2\left(1+\frac{R_{nn}(f)}{S_x|H(f)|^2}\right)^2.$$

III. Simulation Results

In this section, we shall perform computer simulations to evaluate the performance of the equalized DMT. As it is usually the case in practice, we shall choose the margin γ_m as a measure of performance. From the analysis of Section II-C, the DMT margin can be calculated as follows

$$\begin{aligned} \gamma_m &\approx \frac{3\gamma_{\text{eff}}\Gamma}{(Q^{-1}(\frac{P_e}{2}))^2} \\ &= \frac{3\gamma_{\text{eff}}}{(Q^{-1}(\frac{P_e}{2}))^2} \frac{SNR_{\text{geom}}}{\left(2^{\frac{b_{DMT}}{\bar{N}}}-1\right)} \\ &= \frac{3\gamma_{\text{eff}}}{(Q^{-1}(\frac{P_e}{2}))^2} \frac{SNR_{\text{geom}}}{\left(2^{\frac{R_{DMT}N}{f_s\bar{N}}}-1\right)}. \end{aligned} \tag{13}$$

In our simulations, we considered the eight carrier-serving-area (CSA) loops [15] whose configuration is shown in Fig. 3. It is worth mentioning that some of these loops have bridged taps and multiple gauge changes which increase the severity of the channel characteristics.

The simulation parameters used are typical of the high-bit-rate digital subscriber loop (HDSL) environment. More specifically, the two-sided AWGN psd is equal to -113 dBm/Hz

[3] In fact, there is no need for the equalizer as the blocklength becomes infinite since the effect of the cyclic prefix overhead becomes negligible.

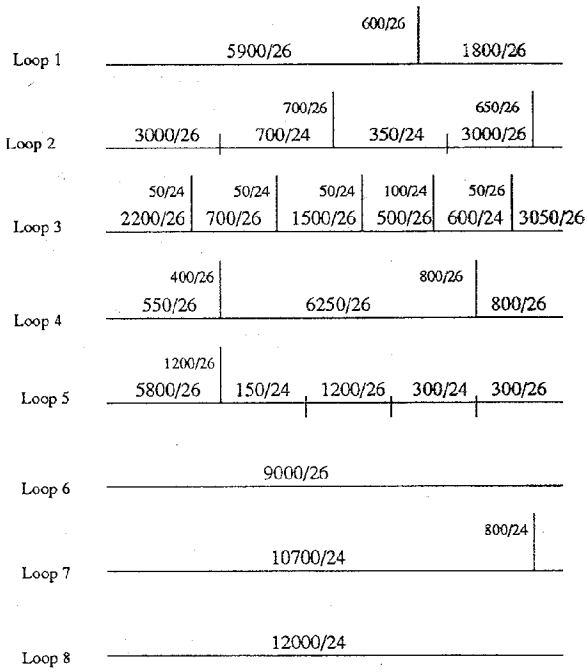

Fig. 3. Configuration of the 8 CSA HDSL loops under study (length (in ft.)/gauge).

and near-end crosstalk (NEXT) is modeled by the transfer characteristics $|H_{\text{NEXT}}(f)|^2 = k_{\text{NEXT}} f^{\frac{3}{2}}$ with $k_{\text{NEXT}} = 10^{-13}$ (corresponding to a 50-pair cable). The target bit rate is 800 kbps, the input power level is 14 dBm (equally distributed across the entire Nyquist bandwidth), the symbol error rate is fixed at 10^{-7} across the subchannels, and a coding gain of 4.2 dB is assumed.

The chosen FFT size for the DMT is 128. The TEQ is assumed to have $N_f = 16$ taps and the memory of the TIR is $N_b = 4$. For the geometric TEQ, we chose the maximum allowable MSE level to be -17 dB, the initial condition for the TIR to be equal to $\frac{1}{\sqrt{N_b+1}}[1 \quad \cdots \quad 1]$, and the delay was not optimized but rather set equal to the optimum delay of the MMSE-UEC equalizer.

In Tables I–IV, we list the achievable margin of the DMT on the 8 CSA loops when equalized by the geometric or the MMSE-UEC TEQ's for sampling frequencies of 384, 416, 448, and 480 kHz, respectively.[4] For comparison purposes, we also calculated the upperbound on margin under the ideal assumption of an infinite blocklength and optimized transmission bandwidth that was derived in Section II-E and a lower bound on margin when no equalizer is used (i.e., a cyclic prefix of length ν is assumed).

Comments:

1) It is clear that the use of equalization results in a substantial margin improvement over the case of no equalization. An additional increase in margin is achieved by designing the equalizer based on the geometric SNR criterion as opposed to the MSE criterion, as it is further demonstrated in Fig. 4 for the sampling frequency $f_s = 448$ kHz.
2) The amount of margin improvement because of equalization and the margin loss with respect to theoretical performance limits differ from one loop to the other. For example, the use of the geometric TEQ brought us to within 2.38 dB from the theoretical bound for Loop 5 at $f_s = 480$ kHz. We believe that yet an appreciable portion of this remaining margin gap can be bridged using the measures that will be outlined in Section IV.

[4]These sampling frequencies correspond to multicarrier symbol rates ($\frac{1}{T}$) of 3, 3.25, 3.5, and 3.75 kHz, respectively.

TABLE I
COMPARISON BETWEEN THE MARGIN (IN dB) OF THE DMT UNDER THE CONDITIONS OF INFINITE BLOCKLENGTH, NO TEQ AND EQUALIZED BY THE GEOMETRIC AND MMSE-UEC TEQ'S FOR THE 8 CSA HDSL LOOPS AT A SAMPLING FREQUENCY OF 384 kHz (THE CALCULATED LOSSES (IN dB) ARE WITH RESPECT TO THE INFINITE-BLOCKLENGTH CASE)

Loop No.	Infinite Blocklength		Geometric TEQ		MMSE-UEC TEQ		No TEQ	
	B.W. (kHz)	γ_m	γ_m	Loss	γ_m	Loss	γ_m	Loss
1	180	10.67	7.66	3.01	6.60	4.07	3.42	7.25
2	158	11.52	7.91	3.60	6.98	4.54	3.97	7.55
3	214	10.30	7.41	2.89	6.14	4.16	3.00	7.30
4	154	8.84	5.14	3.69	4.57	4.26	1.12	7.72
5	256	9.67	6.39	3.28	5.08	4.59	1.72	7.95
6	210	8.79	5.76	3.03	4.71	4.08	1.29	7.50
7	158	10.45	6.75	3.70	6.00	4.44	2.61	7.84
8	200	10.25	7.37	2.88	6.11	4.14	2.81	7.43

TABLE II
COMPARISON BETWEEN THE MARGIN (IN dB) OF THE DMT UNDER THE CONDITIONS OF INFINITE BLOCKLENGTH, NO TEQ AND EQUALIZED BY THE GEOMETRIC AND MMSE-UEC TEQ'S FOR THE 8 CSA HDSL LOOPS AT A SAMPLING FREQUENCY OF 416 kHz (THE CALCULATED LOSSES (IN dB) ARE WITH RESPECT TO THE INFINITE-BLOCKLENGTH CASE)

Loop No.	Infinite Block Length		Geometric TEQ		MMSE-UEC TEQ		No TEQ	
	B.W. (kHz)	γ_m	γ_m	Loss	γ_m	Loss	γ_m	Loss
1	180	10.67	7.57	3.10	6.72	3.95	3.52	7.15
2	158	11.52	7.47	4.05	6.87	4.65	3.66	7.86
3	214	10.30	7.81	2.49	6.52	3.78	3.37	6.93
4	154	8.84	5.07	3.77	4.60	4.23	.96	7.88
5	256	9.67	6.97	2.70	5.52	4.16	2.08	7.60
6	210	8.79	6.04	2.75	5.07	3.73	1.66	7.13
7	158	10.45	6.53	3.91	5.89	4.56	2.36	8.09
8	200	10.25	7.65	2.60	6.52	3.72	3.13	7.12

TABLE III
COMPARISON BETWEEN THE MARGIN (IN dB) OF THE DMT UNDER THE CONDITIONS OF INFINITE BLOCKLENGTH, NO TEQ AND EQUALIZED BY THE GEOMETRIC AND MMSE-UEC TEQ'S FOR THE 8 CSA HDSL LOOPS AT A SAMPLING FREQUENCY OF 448 kHz (THE CALCULATED LOSSES (IN dB) ARE WITH RESPECT TO THE INFINITE-BLOCKLENGTH CASE)

Loop No.	Infinite Blocklength		Geometric TEQ		MMSE-UEC TEQ		No TEQ	
	B.W. (kHz)	γ_m	γ_m	Loss	γ_m	Loss	γ_m	Loss
1	180	10.67	7.42	3.25	6.68	4.00	3.46	7.21
2	158	11.52	6.98	4.54	6.46	5.06	3.05	8.46
3	214	10.30	7.78	2.52	6.73	3.57	3.70	6.60
4	154	8.84	5.06	3.78	4.58	4.26	.98	7.86
5	256	9.67	7.16	2.51	6.04	3.63	2.60	7.07
6	210	8.79	6.05	2.75	5.24	3.55	1.89	6.90
7	158	10.45	6.46	3.98	5.78	4.66	2.34	8.10
8	200	10.25	7.75	2.50	6.72	3.52	3.40	6.85

3) Other factors that control the margin difference between the 4 studied cases are the values of N_f, N_b, N, input power, $MSE_{\max}$, and f_s. The choice of N_f represents a tradeoff between complexity and performance (ability of the equalizer to satisfy the MSE constraint). Similarly, while choosing N_b too small reduces the bit rate loss due to cyclic prefix, the resulting equalization MSE with a length-N_f equalizer might be much higher than its maximum allowable value of $MSE_{\max}$. Increasing the FFT size N brings the performance of the equalized DMT closer to the upperbound of Section II-E, nevertheless, could result in a prohibitive implementation cost. Concerning the effect of the input power, we must always keep in mind that increasing it beyond a certain level is useless because of the presence of crosstalk. Choosing the maximum allowable MSE level, $MSE_{\max}$, represents a compromise between having a cost-effective TEQ that can meet it and achieving acceptable performance in the sense that the equalized CIR closely resembles the calculated TIR. Finally, choosing the sampling frequency (which is equal to twice the transmission bandwidth in our case since we assume that $\bar{N} = \frac{N}{2}$) outside of a certain range could result in an appreciable margin loss, as depicted in Fig. 5. Ideally, the sampling frequency should be high enough and the transmission bandwidth (or equivalently $\bar{N}$) is jointly optimized with b, on a per-loop basis, to maximize the margin (c.f. Section IV-A).
4) In all of our simulations, we have found that, at the optimum TIR, the MSE inequality constraint is met with equality. This means that the solution of our non-linear constrained optimization problem lies on the boundary of the feasible region. This observation further consolidates our earlier argument that minimizing MSE of the TEQ does not necessarily maximize SNR_{geom}.
5) To illustrate further the action of the geometric TEQ, we have plotted in Fig. 6 the magnitude responses of the optimum TIR's of the geometric and MMSE-UEC TEQ's together with that of the original CIR (normalized to have unit energy). It is clear that the amplitude response of the optimum TIR of the geometric TEQ very closely resembles that of the original CIR, with the important advantage that it has a much shorter impulse response duration.
6) Finally, a few words about the complexity-performance tradeoffs are in order. In our simulations, the performance improvement of the geometric TEQ over the MMSE-UEC TEQ is achieved with both equalizers having the same number of taps. Furthermore, the optimal settings of both equalizers are calculated (from their corresponding TIR's) using (2), hence both require the same computational complexity. However, the main difference in the complexity of the two equalization schemes lies in the algorithm used to compute the optimum TIR settings. Under the MMSE-UEC criterion, they are computed by solving a constrained *convex* quadratic programming problem that has a *unique global optimum*. On the other hand, under the geometric SNR criterion, we need to solve a constrained nonlinear programming problem that does not have a unique global optimum in general; this is the price paid for the improvement in performance.

TABLE IV
COMPARISON BETWEEN THE MARGIN (IN dB) OF THE DMT UNDER THE CONDITIONS OF INFINITE BLOCKLENGTH, NO TEQ AND EQUALIZED BY THE GEOMETRIC AND MMSE-UEC TEQ'S FOR THE 8 CSA HDSL LOOPS AT A SAMPLING FREQUENCY OF 480 kHz (THE CALCULATED LOSSES (IN dB) ARE WITH RESPECT TO THE INFINITE-BLOCKLENGTH CASE)

Loop No.	Infinite Block Length		Geometric TEQ		MMSE-UEC TEQ		No TEQ	
	B.W. (kHz)	γ_m	γ_m	Loss	γ_m	Loss	γ_m	Loss
1	180	10.67	7.23	3.43	6.62	4.04	3.27	7.40
2	158	11.52	6.68	4.84	6.06	5.46	2.65	8.87
3	214	10.30	7.88	2.42	6.90	3.39	3.92	6.37
4	154	8.84	5.07	3.77	4.73	4.11	.89	7.94
5	256	9.67	7.29	2.38	6.37	3.30	2.92	6.76
6	210	8.79	6.08	2.71	5.41	3.39	1.94	6.85
7	158	10.45	6.45	3.99	5.88	4.57	2.35	8.09
8	200	10.25	7.50	2.75	6.74	3.51	3.30	6.95

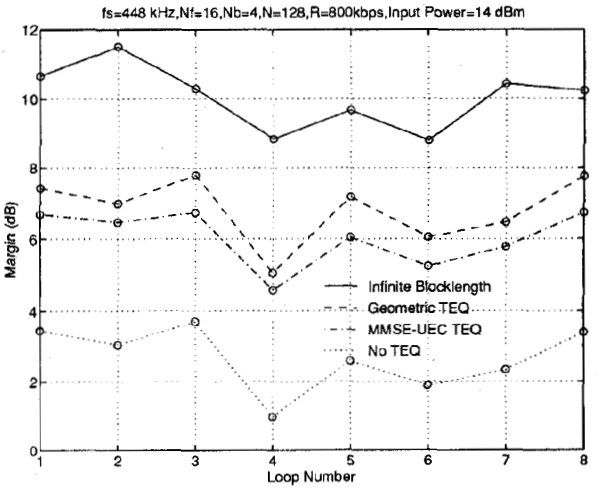

Fig. 4. Margin of the DMT for the 8 CSA loops with and without equalization for a sampling frequency of 448 kHz.

IV. RELATED ISSUES AND FUTURE RESEARCH

In this section, we briefly explore several measures to enhance further the performance of the equalized DMT by relaxing some of the assumptions made in this paper. These measures are currently under investigation and will be reported in future publications.

A. Optimization of the Transmission Bandwidth

An important component of optimizing the performance of the DMT is bandwidth optimization. Typically, the sampling frequency is chosen high enough to include the maximum anticipated transmission bandwidth. Then, bandwidth optimization algorithms of the type discussed in [9] are applied to determine the optimum number of subchannels that should be used out of the $\frac{N}{2}$ available ones to, say, maximize the margin.

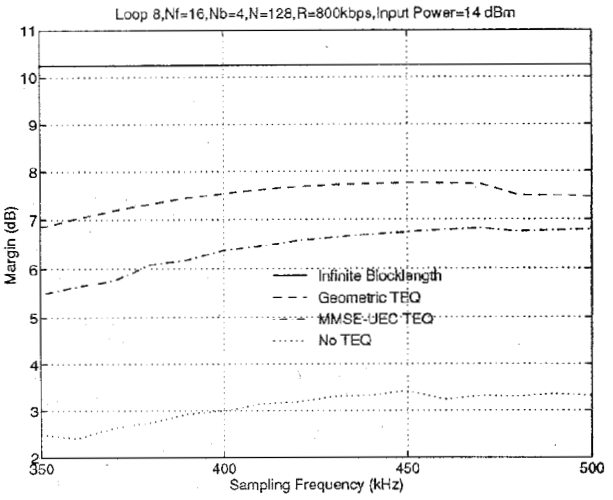

Fig. 5. Variation of the DMT margin with the sampling frequency for Loop 8.

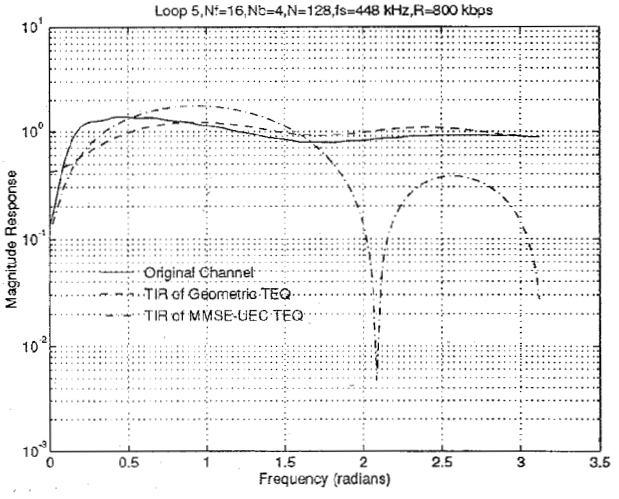

Fig. 6. Magnitude responses of the optimum TIR's of the geometric and MMSE-UEC TEQ's together with that of the original CIR (normalized to have unit energy).

Subchannels whose signal-to-noise ratio can not support a specified minimum number of bits are excluded.

In this paper, we assumed for simplicity that all $\frac{N}{2}$ subchannels are used, i.e., no bandwidth optimization was performed. A higher margin for the equalized DMT can be achieved by jointly optimizing the TIR coefficients b and the transmission bandwidth $(= \frac{\bar{N}}{T})$ to maximize (13). Note that when the transmission bandwidth is allowed to vary (through the optimization of $\bar{N}$), then optimizing the margin of the DMT transceiver is not necessarily equivalent to maximizing the geometric SNR, as it can be easily verified from (13). Stated differently, maximizing SNR_{geom} is equivalent to maximizing the channel throughput (in b/symbol) which also maximizes the bit rate, at a fixed transmission bandwidth. However, there could be another $(\mathrm{b}, \bar{N})$ combination that results in a higher bit rate by achieving an optimum compromise between the channel throughput and the bandwidth [3].

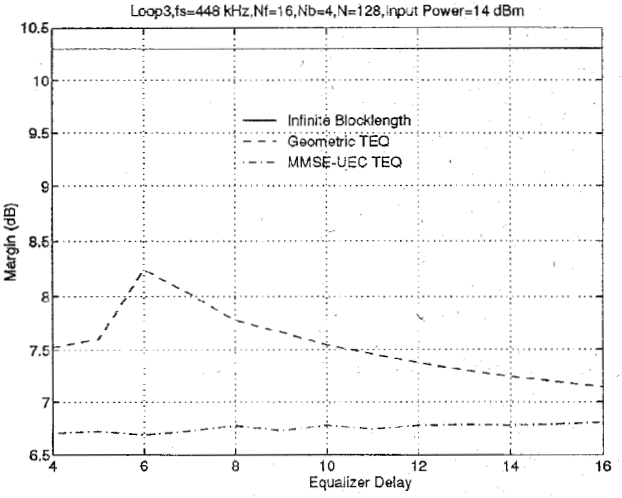

Fig. 7. Variation of the DMT margin with the equalizer delay for Loop 3.

B. Choice of the Equalizer Delay

For the MMSE-UEC TEQ, a characterization of the unique optimum delay was given in [4]. There, it was also demonstrated that choosing the delay outside of a certain range around the optimum value could result in a significant performance degradation. For the geometric TEQ, determining the optimum delay is more difficult since the effect of the delay Δ appears only in the inequality constraint $\mathrm{b}^* \mathrm{R}_\Delta \mathrm{b} \leq MSE_{max}$. In this paper, we have set the delay of the geometric TEQ equal to the optimum delay of the MMSE-UEC TEQ, which might not be the optimum choice. Optimization of the delay could result in a further improvement in the performance of the geometric TEQ over that of the MMSE-UEC TEQ. To illustrate this point, we have plotted in Fig. 7 the variation of the margin of the DMT with the delay for both the geometric and the MMSE-UEC TEQ's. For the given scenario, choosing the delay of the geometric TEQ to be equal to the optimum delay of the MMSE-UEC TEQ (which we determined to be 8) results in a 0.47 dB margin loss from the optimum margin achieved at $\Delta = 6$.

C. Choice of the Initial Condition

For our constrained nonlinear optimization problem, the choice of the initial condition affects the optimum TIR as computed by the iterative numerical search procedure. In our simulations, we have found that the normalized all-ones vector $\frac{1}{\sqrt{N_b+1}}[1 \quad \cdots \quad 1]$ is a good initial condition. However, it might be necessary to compare the achievable margin with a number of different initial conditions to improve performance.

As an example, we have listed in Table V the calculated "optimum" TIR's for different initial conditions for $f_s = 448$ kHz on loop 1 and their corresponding geometric SNR's and margins.

It can be seen from the table that using the unit vector $[1 \quad 0 \quad \cdots \quad 0]$ as an initial condition instead of the all-ones vector results in a DMT margin loss of 0.79 dB. It is also interesting to note that completely different settings for the TIR could result in very close DMT margin values.

TABLE V
EFFECT OF THE INITIAL CONDITION ON THE GEOMETRIC SNR AND MARGIN (BOTH IN dB) OF THE GEOMETRIC TEQ FOR CSA HDSL LOOP 1 AT A SAMPLING FREQUENCY OF 448 kHz

Initial Condition for b					Optimum TIR for Geometric TEQ					SNR_{geom}	γ_m
b_0	b_1	b_2	b_3	b_4	b_0	b_1	b_2	b_3	b_4		
$\frac{1}{\sqrt{5}}$	$\frac{1}{\sqrt{5}}$	$\frac{1}{\sqrt{5}}$	$\frac{1}{\sqrt{5}}$	$\frac{1}{\sqrt{5}}$	−0.2781	0.0501	−0.5136	0.5075	0.6315	23.53	7.42
1	0	0	0	0	0.9192	−0.0778	−0.2861	−0.1585	−0.2048	22.74	6.63
$\frac{1}{\sqrt{5}}$	$-\frac{1}{\sqrt{5}}$	$\frac{1}{\sqrt{5}}$	$-\frac{1}{\sqrt{5}}$	$\frac{1}{\sqrt{5}}$	0.7944	−0.3189	−0.4020	−0.2327	−0.2269	23.60	7.48
$\frac{1}{\sqrt{2}}$	$\frac{1}{\sqrt{2}}$	0	0	0	0.6220	0.4485	−0.5718	−0.0024	−0.2916	22.76	6.64
0	0	0	0	1	−0.1847	−0.1226	−0.2101	−0.0376	0.9515	23.52	7.41
0	$\frac{1}{\sqrt{2}}$	$\frac{1}{\sqrt{2}}$	0	0	−0.5294	−0.2297	0.7392	0.0636	0.3414	23.60	7.48
$\frac{1}{\sqrt{5}}$	$\frac{1}{\sqrt{5}}$	$\frac{1}{\sqrt{5}}$	$-\frac{1}{\sqrt{5}}$	$-\frac{1}{\sqrt{5}}$	0.3136	0.0618	0.6980	−0.2925	−0.5702	22.84	6.73
0	0	1	0	0	-0.5294	−0.2297	0.7392	0.0636	0.3414	23.60	7.48

D. Pole-Zero Implementation of the Equalizer

Another promising technique to improve further the performance of the equalized DMT toward the theoretical performance upperbound of infinite blocklength is to increase the number of equalizer taps. While it is not clear whether the geometric SNR should be a monotonically increasing function of N_f, it can be easily shown that $\frac{1}{MSE}$ is. Therefore, increasing N_f allows us to decrease N_b while still satisfying the MSE constraint $\mathbf{b}^*\mathbf{R}_\Delta\mathbf{b} \leq MSE_{\max}$. In fact, $MSE_{\max}$ could be made even smaller than its value of -17 dB assumed throughout this paper. The resulting reduction in the value of N_b reduces the data rate loss due to cyclic prefix overhead, thus improving the DMT performance.

In order to avoid the high implementation cost that could result when implementing long FIR equalizers, we propose to use the algorithm that we derived in [5] to convert long FIR equalizers to stable pole-zero equalizers with much fewer taps.

E. Other Constraints

In this work, we sought to maximize the geometric SNR of the DMT subject to a unit-energy constraint on the TIR and a maximum allowable MSE of the equalizer. Several other optimization problems are also possible and are worth investigating since they might result in TIR's that yield better margins than the ones we have obtained here. We list some of these alternative optimization problems next:

1) Maximize SNR_{geom} subject to a unit-tap constraint (UTC) on b, i.e., $b_i = 1$ $(1 \leq i \leq N_b + 1)$ and a maximum allowable equalizer MSE.
2) Minimize MSE of the equalizer subject to either UTC or UEC and a minimum allowable geometric SNR (needed to achieve a prescribed margin for the DMT).
3) Maximize a weighted sum of SNR_{geom} and $\frac{1}{MSE}$ subject to either UTC or UEC.
4) Impose a linear-phase constraint on the TIR to reduce phase distortion by requiring symmetry of the TIR around its middle sample.

V. CONCLUSION

In this paper, we showed that the optimum finite-complexity equalization criterion for the DMT is maximizing the geometric SNR, assuming that the transmission bandwidth is fixed. The problem of computing the optimum target impulse response of a given length was formulated as a constrained nonlinear optimization problem and solved using well-known iterative numerical techniques.

Furthermore, computer simulations on a set of CSA HDSL loops illustrated that the performance of the DMT with the geometric equalizer is better than that achieved with the previously-used MSE equalizer. Presently, we believe that the geometric-equalizer-DMT combination represents a serious step toward approaching theoretical performance limits with a practical implementation cost. Finally, additional measures to improve further the performance of the equalized DMT, that are currently under investigation, were described.

REFERENCES

[1] *Optimization Toolbox Manual*, MATLAB Software Package Version 4.1. The MathWorks, Inc., Natick, MA, 1992.
[2] N. Al-Dhahir and J. Cioffi, "Fast algorithms for the computation of the FIR MMSE-DFE," in *IEEE Int. Conf. Acoust., Speech, Signal Processing*, Mar. 1992, pp. IV533–IV536.
[3] ——, "Bandwidth optimization for combined equalization and coding transceivers with emphasis on the MMSE-DFE," in *IEEE Milcom*, vol. 2, Oct. 1993, pp. 471–475.
[4] ——, "A low-complexity pole-zero MMSE equalizer for ML receivers," in *Proc. Allerton Conf. Commun., Control, Comput.*, Sept. 1994, pp. 623–632.
[5] N. Al-Dhahir, A. H. Sayed, and J. Cioffi, "A high-performance cost-effective pole-zero MMSE-DFE," in *Proc. Allerton Conf. Commun., Control, Comput.*, Sept. 1993, pp. 1166–1175.
[6] J. Chow and J. Cioffi, "A cost-effective maximum likelihood receiver for multicarrier systems," in *Int. Conf. Commun., Chicago*, June 1992, pp. 948–952.
[7] J. Chow, J. Cioffi, and J. Bingham, "Equalizer training algorithms for multicarrier modulation systems," in *Int. Conf. Commun., Geneva*, May 1993, pp. 761–765.
[8] J. Chow, J. Tu, and J. Cioffi, "A discrete multitone transceiver system for HDSL applications," *IEEE J. Select. Areas Commun.*, vol. 9, no. 6, pp. 895–908, Aug. 1991.
[9] P. Chow, "Bandwidth optimized digital transmission techniques for spectrally shaped channels with impulse noise," Ph.D. dissertation, Stanford Univ., Palo Alto, CA, May 1993.
[10] J. Cioffi, G. Dudevoir, M. Eyuboglu, and G. D. Forney Jr., "Minimum mean-square-error decision feedback equalization and coding—Parts I and II," *IEEE Trans. Commun.*, vol. 43, no. 10, pp. 2582–2604, Oct. 1995.
[11] D. Falconer and F. Magee, "Adaptive channel memory truncation for maximum likelihood sequence estimation," *Bell System Tech. J.*, vol. 52, no. 9, pp. 1541–1562, Nov. 1973.
[12] P. Gill, W. Murray, and M. Wright, *Practical Optimization*. London: Academic, 1981.
[13] S. Kasturia, J. Aslanis, and J. M. Cioffi, "Vector Coding for Partial-Response Channels," *IEEE Trans. Inform. Theory*, vol. 36, no. 4, pp. 741–762, July 1990.
[14] E. Lee and D. Messerschmitt, *Digital Communication*. Norwell, MA: Kluwer, 1988.

[15] K. Sistanizadeh, "Loss characteristics of the proposed canonical ADSL loops with 100-Ohm termination at 70, 90, and 120°F," ANSI T1E1.4 Committee Contribution, no. 161, Nov. 1991.

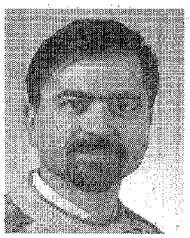

Naofal Al-Dhahir (S'89–M'90) received the B.Sc. degree from Kuwait University with first-class honors in 1989 and the M.Sc. and Ph.D. degrees from Stanford University, in 1990 and 1994, respectively, all in electrical engineering.

He was an Instructor at Stanford University during Winter 1993. Since August 1994, he has been with GE Corporate R&D Center in Schenectady, NY. His research interests are in combined equalization and coding transceivers, fast signal processing algorithms in communications, and satellite communication systems.

John M. Cioffi (S'77–M'78–SM'90) received the B.S.E.E. degree in 1978 from the University of Illinois, and the Ph.D. degree in electrical engineering in 1984 from Stanford University.

He was employed by Bell Laboratories, Holmdel, NJ, from 1978 to 1984, and by IBM Research, San Jose, CA, from 1984 to 1986. He has been on the Stanford faculty since 1986 and is now Chief Technical Officer at Amati Communications Corporation, a company he founded in 1990. His interests are in data transmission and storage.

He is recipient of the 1991 *IEEE Communications Magazine* best paper award and of the 1992 IEEE ISSCC panel speaker award. He was an NSF Presidential Investigator from 1987 to 1992.